Preparation of NaX zeolite films for the sorption of Pb²⁺, Cd²⁺ and Cu²⁺

Chunxiu Zhang[a,b], Huasheng Xu[a,b], Jinpeng Yu[a,b], Pengfei Wang[a,b],*

[a]*Shanghai Research Institute of Chemical Industry, Shanghai 200062, China, Tel. +86 13122369851,*
email: m18376654611@163.com (C. Zhang), Tel. +86 13917611405, email: xhs69@163.com (H. Xu), Tel. +86 13501826084,
email: freeyujinpeng@126.com (J. Yu)
[b]*Shanghai Luqiang New Materials Co. Ltd., Shanghai 201806, China, Tel. +86 021 52815377-0101, Fax +86 021 52802532,*
email: wpf@sricims.com (P. Wang)

ABSTRACT

NaX zeolite films, used as an effective sorbent for Pb²⁺, Cd²⁺ and Cu²⁺ from aqueous solution, were prepared on α-Al₂O₃ ceramic tube by pre-coating sol, drying in warm temperature and crystallizing in synthetic solution. The resulting films were characterized with X-ray diffractometer (XRD), scanning electron microscopy (SEM), energy dispersive spectrometer (EDS) and sorption test. Results showed that a thin NaX zeolite film with a thickness of 1–3 μm was obtained. The effects of initial pH, concentration, and sorption time on film sorption capacity for Pb²⁺, Cd²⁺ and Cu²⁺ were investigated. It was observed that the sorption isotherms of NaX zeolite films were all well described by the Langmuir isotherm model. The saturation sorption capacities of Pb²⁺, Cd²⁺, Cu²⁺ on the films were increasing with temperature between 25–45°C, which were 3.075 mmol/L, 2.992 mmol/L and 2.274 mmol/L at 45°C, respectively. In addition, the sorption rates of NaX zeolite films were studied in comparison with pelletized NaX zeolite particles based on sorption kinetic models: Lagergren pseudo-first-order model, Lagergren pseudo-second-order model and Weber and Morris model. The models indicated that NaX zeolite film can effectively avoid the effect of diffusion resistance caused by particle morphology due to increasing external surface area.

Keywords: Sorption; NaX zeolite; Film; Heavy metal; Kinetic

1. Introduction

Heavy metals of industrial wastewater, discharged from iron ore mining, alloy smelting and metal finishing, have caused serious threat to ecosystems, especially to human beings and animals because of their high toxicity [1], carcinogenicity [2] and non-biodegradablity [3]. For instance, Pb primarily accumulates in muscles, bones, kidneys, and brain tissues, which can result in anemia, nervous system disorders, and kidney disease [4]. Cd in living organisms can lead to many symptoms including hypertension, respiratory disorder, and damage to the kidneys and liver [2]. The presence of excessive Cu in water can be harmful to the living organisms, such as lung cancer, stomach upset, headache, dizziness, and respiratory distress [5].

There are several methods to remove heavy metals from industrial wastewater, including chemical precipitation [6], oxidation reduction [7], electrolysis [8], ion exchange [9], and sorption [3,10]. Among these methods, sorption is considered to be one of the most effective methods for wastewater treatment due to its low cost and high efficiency [11]. Natural materials, derived from agricultural waste, industrial by-product or modified biopolymers, are common adsorbents. But low selectivity and production of waste products of these adsorbents are the major drawback [12]. NaX zeolite, a kind of silica alumina crystal with microporous structure and high specific surface area [13], has shown high sorption capacity for heavy metal and regeneration ability [2], which is widely used in industrial wastewater treatment.

NaX zeolite powder in the market is commonly micrometer-scale particles. It may result in excessive pressure drops when directly applied in fixed bed or any other

*Corresponding author.

flow-through systems [14]. Thus, NaX zeolite powder is often made into millimeter-scale pelletized particles before using. But this would lead to another problem-intraparticle diffusion. The sorption process may be impeded by intraparticle diffusion more and more with the pelletized NaX zeolite particle size increasing. Barros [15] considered intraparticle diffusion as one of the rate-controlling step of the sorption process for NaX zeolite in the fixed bed column during removal process of Cr(III). Pepe [16] also reported that internal and external mass transfer resistances played a key role in heavy metals removal process on fixed bed padding 0.30–0.60 mm natural zeolites. Therefore, developing NaX zeolite materials with good solid-liquid contact to achieve desired sorption effect has attracted more and more attention.

Considering the advantage of increasing surface area for mass transfer, it is essential to make zeolite into thin film. The zeolite film can accelerate the sorption rate as large external surface area, which would show good potential in adsorbing heavy metals, ammonium compounds, oxygenates, etc. There are several methods to prepare zeolite film [17–20], of which the secondary growth method [21] is the most common one. Crystal seed plays an important role in the secondary growth method but its preparation process is complex. To simplify the secondary growth method, we attempt to substitute crystal seed with aluminosilicate sol. The aluminosilicate sol, as synthetic substance of zeolite film, is coated on the ceramic tube, then pretreated in warm temperature. Subsequently, the ceramic tube with sol dry layer is placed in synthetic solution to form zeolite film. This new method would be more simple, with higher potential to industrialization.

In the study, NaX zeolite films were synthesized on α-Al$_2$O$_3$ ceramic tube by pre-coating sol, drying in warm temperature and crystallizing in synthetic solution, and then they were used to absorb Pb^{2+}, Cd^{2+}, Cu^{2+} from aqueous solution. The sorption isotherm of NaX zeolite films was evaluated by Langmuir model and Freundlich model. Compared with pelletized NaX zeolite particles, kinetic parameters of NaX zeolite films were estimated using the Lagergren pseudo-first-order model, Lagergren pseudo-second-order model, and Weber and Morris model. The results obtained from this study could provide better insight in the sorption process of heavy metals on NaX zeolite films.

2. Materials and methods

2.1. Materials

Sodium aluminate (CP), sodium hydroxide (AR), sodium silicate (AR) were obtained from Shanghai Zhanyun Chemical Co. Ltd. (China). Porous α-Al$_2$O$_3$ ceramic tubes (12 mm outside diameter, 8 mm inside diameter, 50 mm length, 2–5 µm pore size, 38% average porosity) were purchased from Zibo Dongqiang Environmental Protection Equipment Co. Ltd. (China). Pelletized NaX zeolite particles (80 wt.% NaX zeolite, 0.8–1.25 mm particle diameter) were provided by Shanghai Luqiang New Materials Co. Ltd. (China). Pb(NO$_3$)$_2$ (AR), Cd(NO$_3$)$_2$·4H$_2$O (AR) and CuSO$_4$·5H$_2$O (AR) were purchased from Sigma-Aldrich.

2.2. Methods

2.2.1. Film preparation

Film preparation with pre-coating sol: NaX zeolite film grew hydrothermally on the surface of the porous α-Al$_2$O$_3$ ceramic tube support. The α-Al$_2$O$_3$ ceramic tube was polished with 400# SiC sandpaper. In order to remove adhesive impurity substance on the supports, it was dipped into 10% HNO$_3$ solution and 10% NaOH solution for 2 h, successively. After washing with deionized water, the α-Al$_2$O$_3$ ceramic tube was dried in air and calcined at 400°C for 2 h.

Aluminosilicate sol was prepared by mixing sodium aluminate, sodium silicate, sodium hydroxide and deionized water in the molar ratio of 1.0 Al$_2$O$_3$·3.5 SiO$_2$·7.9 Na$_2$O·630 H$_2$O, and stirred continuously at room conditions for 30 min. Pre-coating sol steps were as follows: The one end of α-Al$_2$O$_3$ ceramic tube was blocked by Teflon cap, and the other end was connected with vacuum pump, which was controlled to 0.01 MPa for 5 s after ceramic tube immersed in the aluminosilicate sol. Then the α-Al$_2$O$_3$ ceramic tube was taken out, and aluminosilicate sol on outside surface of support was obtained. It was essential to treat the α-Al$_2$O$_3$ ceramic tube in 35°C oven for 18 h. Subsequently, the α-Al$_2$O$_3$ ceramic tube with pre-coating sol was vertically placed in a Teflon-lined stainless steel autoclave, and then the fresh synthesis solution with same molar ratio as above aluminosilicate sol was poured into the autoclave. After ageing process at 70°C for 6 h and crystallization process at 100°C for 12 h, the NaX zeolite film was achieved. The film was washed with deionized water for five times. For further application, the NaX zeolite film was dried in 35°C oven night and calcined at 400°C for 2 h with 1°C/min heating rate.

Film preparation without pre-coating sol: The procedure described above, without the pre-coating sol steps, was followed.

2.2.2. Film characterization

The crystal structure of NaX zeolite films was detected with XRD (D8 ADVANCE, BRUKER) using Cu Kα radiation with operating pressure at 45 kV and scanning rate of 2° min^{-1} over a 2θ range of 5° to 50°.

The morphology of NaX zeolite films was characterized by SEM (Merlin Compact, ZEISS). NaX Zeolite films were fractured cryogenically in liquid nitrogen. EDS (Merlin Compact, ZEISS) was used to determine the elemental compositions and the Si/Al ratio of the NaX zeolite films. To avoid the interference from the support, NaX zeolite film was scraped from the support as test sample for EDS.

2.2.3. Batch sorption study

In this study, the sorption of Pb^{2+}, Cd^{2+} and Cu^{2+} on NaX zeolite films was carried out using the batch method. The stock solutions containing concentration of Pb^{2+}, Cd^{2+} and Cu^{2+} within 0–1.5 mmol/L were prepared by dissolving Pb(NO$_3$)$_2$, Cd(NO$_3$)$_2$·4H$_2$O and CuSO$_4$·5H$_2$O in deionized water respectively. Sorption experiments were conducted with 0.02 g/100 ml solid-liquid ratio. The pH value of solutions was adjusted using HNO$_3$ (2%) or NaOH (2%), then

placed the solutions on the rotary shaker with 200 rpm at 25–45°C.

The sorption rate of Pb^{2+}, Cd^{2+} and Cu^{2+} on NaX zeolite films was evaluated compared with pelletized NaX zeolite particles. Pelletized NaX zeolite particles were washed by deionized water for five times, then calcined at 400°C for 2 h. The 100 mL of Pb^{2+} (or Cd^{2+}, Cu^{2+}) solution with initial concentration of 0.05 mmol/L were contacted with 0.02 g NaX zeolite films or 0.025 g NaX zeolite particles (80 wt.% NaX zeolite) for 8 h at 25°C on rotary shaker with 200 rpm.

Concentration of Pb^{2+}, Cd^{2+} and Cu^{2+} was determined by atomic absorption spectrometer with graphite furnace (TAS-990 AFG, Beijing Purkinje General Instrument Co. Ltd.). Sorption capacity q_t of heavy metals on sorbent was calculated using Eq. (1):

$$q_t = \frac{(C_0 - C_t)V}{m} \tag{1}$$

where q_t is the sorption amount of heavy metal on per unit mass of adsorbent at time t (mmol/g), C_o and C_t are the heavy metal concentrations of liquid phase at initial and time t (mmol/L), respectively, V is volume of heavy metal solution (L), m is the amount of NaX zeolite (g).

2.2.4. Sorption isotherm model

Sorption process can be theoretically studied and predicted under constant temperature using sorption isotherm models. Langmuir and Freundlich models are two of the most common models in describing the isothermal sorption process.

The Langmuir isotherm model is used to describe homogeneous monolayer sorption processes. The equation of Langmuir model can be represented as Eq. (2) [22]:

$$q_e = \frac{bQ_oC_e}{1 + bC_e} \tag{2}$$

The linear equation of Langmuir model as following Eq. (3):

$$\frac{C_e}{q_e} = \frac{1}{Q_o b} + \frac{C_e}{Q_o} \tag{3}$$

where q_e is sorption amount of adsorbate on per unit amount adsorbent at equilibrium (mmol/g); C_e is the concentration of adsorbate in solution at equilibrium (mmol/L), Q_o is the maximum sorption capacity (mmol/g), b is the constant representing the sorption affinity between adsorbent and adsorbate (L/mmol).

Freundlich model is applied to describe the sorption data on heterogeneous surface at low and intermediate concentrations [23,24]. The equation of Freundlich model is given as following Eq. (4) :

$$q_e = K_F C_e^n \tag{4}$$

The linear equation of Freundlich model as following Eq. (5):

$$\ln q_e = \ln K_F + n \ln C_e \tag{5}$$

where K_F, and n are the Freundlich constant related to sorption capacity [(mmol/g) (L/mmol)^n] and sorption intensity, respectively.

2.2.5. Sorption kinetics

2.2.5.1. Reaction-based model

Two kinds of reaction-based models, Lagergren pseudo-first-order kinetic model and Lagergren pseudo-second-order kinetic model, were used to analyze experimental data [25–27].

Equation of Lagergren pseudo-first-order kinetic model is expressed in Eq. (6):

$$\frac{dq}{dt} = k_1(q_{e1} - q) \tag{6}$$

Integrating Eq. (6) from $t = 0$ to $t = t$ and $q = 0$ to $q = q_t$ results in:

$$\ln(q_{e1} - q_t) = \ln q_{e1} - k_1 t \tag{7}$$

Equation of Lagergren pseudo-second-order kinetic model is expressed in Eq. (8):

$$\frac{dq}{dt} = k_2(q_{e2} - q)^2 \tag{8}$$

Integrating Eq. (8) from $t = 0$ to $t = t$ and $q = 0$ to $q = q_t$ leads to:

$$\frac{t}{q_t} = \frac{1}{k_2 q_{e2}^2} + \frac{t}{q_{e2}} \tag{9}$$

where q_{e1}, q_{e2} are sorption amount of adsorbate on per unit amount adsorbent at equilibrium (mmol/g), q_{e1} is determined by a nonlinear regression analysis, q_{e2} can get from linear regression analysis; q_t is sorption amount of adsorbate on per unit amount adsorbent at sorption time t (mmol/g); k_1 and k_2 are Lagergren pseudo-first-order kinetic sorption rate constant (min^{-1}) and Lagergren pseudo-second-order kinetic sorption rate constant (g·m mol^{-1}·min^{-1}), respectively.

2.2.5.2. Diffusion-based model

Weber and Morris model is a common diffusion kinetic model, expressed as Eq. (10):

$$q_t = I + K_{WM}\sqrt{t} \tag{10}$$

where K_{WM} is the diffusion rate coefficient (mmol·g^{-1}·min$^{-0.5}$), I is the intercept (mmol/g). It could be employed to examine transport mechanisms of the solute, including intraparticle diffusion and external mass transfer. At $I = 0$, the intraparticle diffusion is considered as the rate-limiting step [26,28–29]. At $I \neq 0$, both intraparticle diffusion and external mass transfer are considered as rate limiting step [30,31].

3. Results and discussion

3.1. Characterization of NaX zeolite film

Fig. 1 Showed the XRD patterns of NaX zeolite films with pre-coating sol (Fig. 1d) and without pre-coating sol (Fig. 1c). It shows that only crystalline phase of α-Al$_2$O$_3$ is observed in Fig. 1c, which suggests that NaX zeolite did not grow on the surface of α-Al$_2$O$_3$ ceramic tube. It was considered the reason of repulsion between support and film precursor material because of their similar surface charges (α-Al$_2$O$_3 \approx -32$ mV and Na-X ≈ -43 mV) [17]. While, the pattern of NaX zeolite film with pre-coating sol exactly matched NaX zeolite powder [32] except characteristic peak of α-Al$_2$O$_3$ in Fig. 1d, which indicated that the NaX zeolite was synthesized on α-Al$_2$O$_3$ ceramic tube. It could
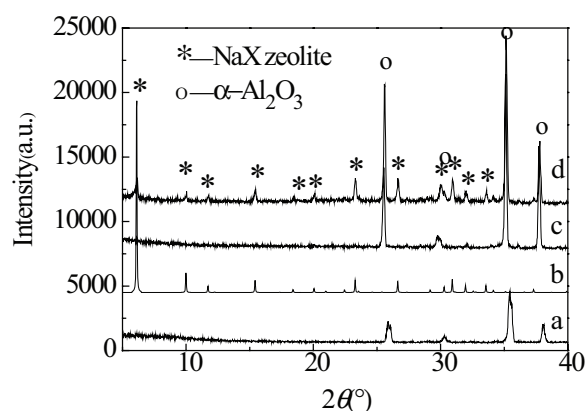

Fig. 1. XRD patterns of α-Al$_2$O$_3$ ceramic tube (a), NaX zeolite powder (b), NaX zeolite film without pre-coating sol (c) and with pre-coating sol (d).

be explained that the pre-coating sol on surface of α-Al$_2$O$_3$ ceramic tube transformed to NaX zeolite film precursor material during polycondensation process, further inducing formation of NaX zeolite film.

The SEM images of α-Al$_2$O$_3$ ceramic tube, surface of NaX zeolite film without pre-coating sol, surface and cross-section of NaX zeolite film with pre-coating sol are presented in Fig. 2. Little zeolite crystal grew on surface of α-Al$_2$O$_3$ ceramic tube without pre-coating sol (Fig. 2b), which was in accordance with result of XRD. While successive and uniform NaX zeolite film on the α-Al$_2$O$_3$ ceramic tube surface was obtained with pre-coating sol (Fig. 2c). Owing to low viscosity of aluminosilicate sol, pre-coating sol on surface of α-Al$_2$O$_3$ ceramic tube spread thinly and successively, which could gradually transformed to crystal nucleus during drying process, leading to cross-linking growth of NaX zeolite film with crystallizing process. The thickness of film was 1–3 µm (Fig. 2d), which was in favor of facilitating mass transfer and accelerating sorption rate as it was thinner than other reported membranes (20–30 µm [21]).

Only O, Na, Al and Si in NaX zeolite film were obtained from the EDS (Table 1). And the Si/Al ratio of the NaX zeolite film is 1.09, is consistent with Si/Al ratio of X type zeolite in the range of 1 to 1.5.

Overall, it was confirmed the formation of a phase-pure NaX zeolite film. Compared with traditional in-situ hydrothermal method [33] and seeded secondary growth method [20], the method in this article could avoid complex preparation process of crystal seed and be easier to operate.

3.2. The pH value

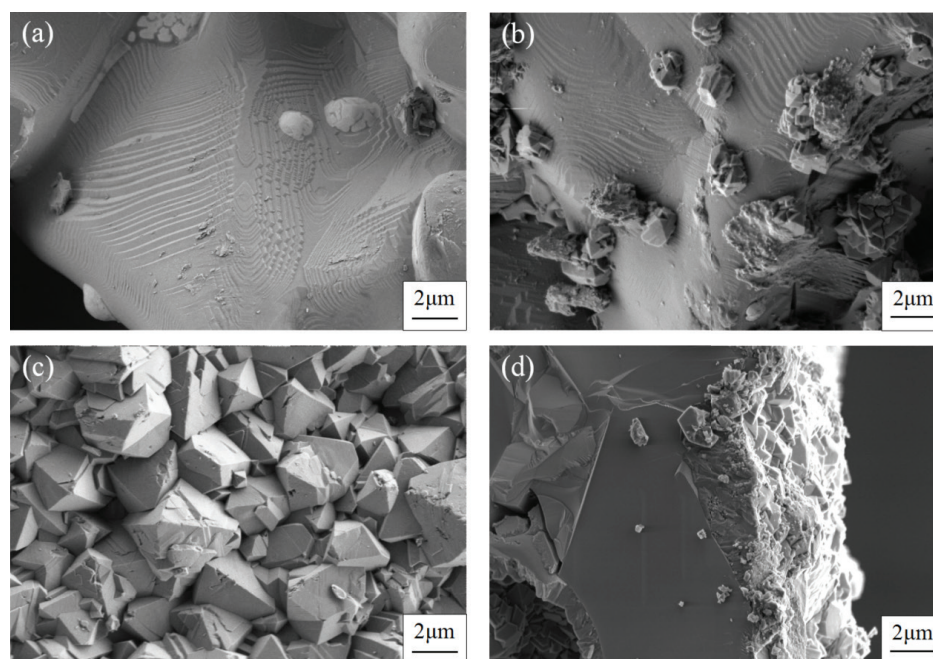The initial pH value of the solution plays an important role on the sorption of Pb^{2+}, Cd^{2+} and Cu^{2+} on NaX zeolite

Fig. 2. SEM images of α-Al$_2$O$_3$ ceramic tube (a), surface of NaX zeolite film without pre-coating sol (b), surface (c) and cross-section (d) of NaX zeolite film with pre-coating sol.

Table 1
Element analysis of NaX zeolite film

Element	The molar percentage (%)
O	64.42
Na	7.29
Al	13.51
Si	14.78
Total	100.00
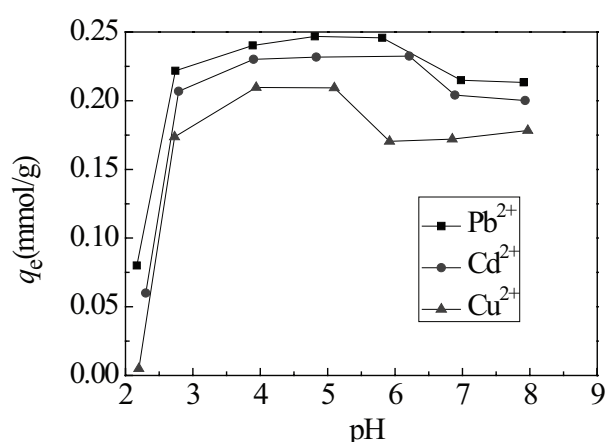
Fig. 3. Sorption of Pb^{2+}, Cd^{2+} and Cu^{2+} on the NaX zeolite films at different pH value (T = 25°C, S/L = 0.2 g/L, t = 8 h and C_0 = 0.05 mmol/L).

films (Fig. 3), due to the pH-dependent of the surface characteristics of the zeolite and ionization degree of the metals in aqueous medium [20,31]. The sorption capacity of Pb^{2+} increased gradually with initial pH value in the region of pH 2.0–4.0 and maintained a high level at pH 4.0–6.0. The increasing of sorption capacity is mainly attributed to ion exchange, as H^+ are competitive to Pb^{2+} for ion exchange sites. At pH 6.0–8.0, the sorption capacity decreased gradually. This may be explained by the hydrolysis of Pb^{2+} in aqueous solution, which have weaker electrostatic attraction with the negatively charged surface of NaX zeolite films. Similar sorption curves of Cd^{2+} and Cu^{2+} on NaX zeolite films were also found. It can be seen that the sorption capacity of Cu^{2+} increased slowly at pH 6.0–8.0. This is because Cu^{2+} begins to precipitate at pH~6.3 with the initial concentration of 0.05 mmol/L (The precipitation constant of $Cu(OH)_2(s)$ is 2.2×10^{-20}). To avoid competitive sorption of H^+ and precipitation formation, the initial pH value of the all heavy metal solution was adjusted to ~5 in the following investigation.

3.3. Concentration

Fig. 4 shows the sorption isotherms of Pb^{2+}, Cd^{2+} and Cu^{2+} from aqueous solution on NaX zeolite films respectively. Sorption capacity of the Pb^{2+} (Fig. 3a) on NaX zeolite film sharply increased in the low concentration, then gradually increased until equilibrium was reached. This is the result that concentration driving force of Pb^{2+} makes sorp-

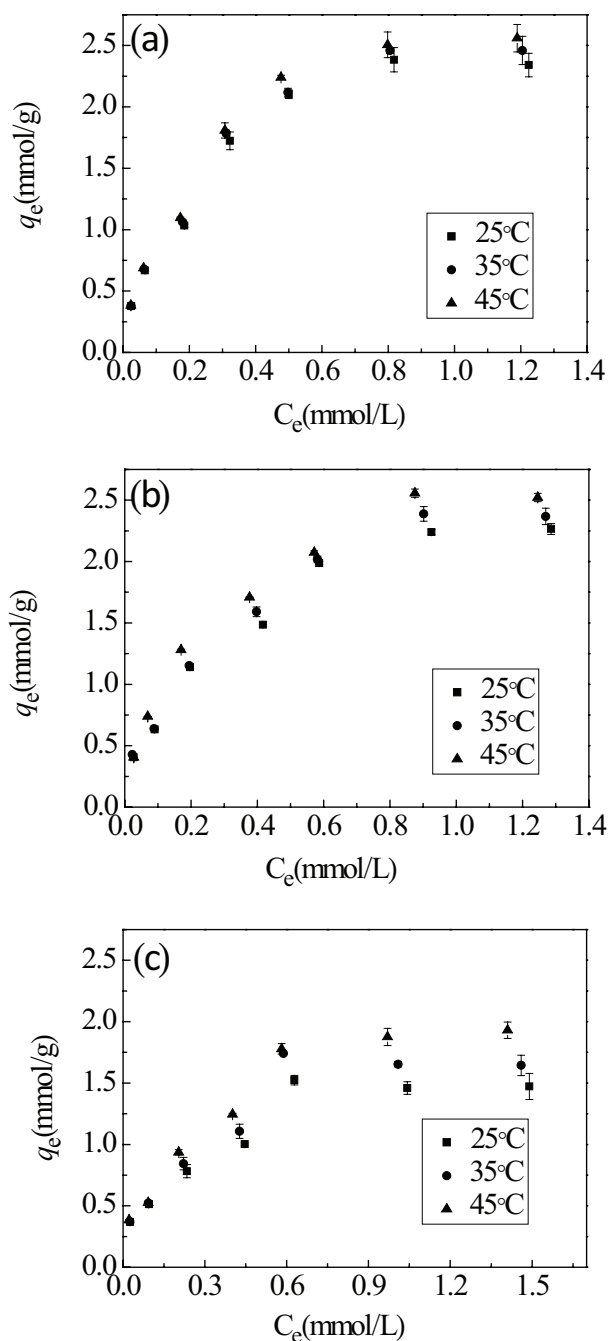Fig. 4. Sorption isotherms of Pb^{2+}(a), Cd^{2+} (b) and Cu^{2+} (c) on the NaX zeolite films (T = 25°C, S/L = 0.2 g/L, t = 3 h and pH = 5).

tion capacity increase [35]. The cationic sites in the channels and cavities of NaX zeolite film are finite [36], so the sorption capacity can't increase when cationic sites are completely saturated. Moreover, the isotherm shape of Pb^{2+} was "L2" type according to Giles classification for isotherms [30,37], which shows that the data had reached a maximum value, resulting in the presence of the plateau. It was speculated that there was weak competition from the water molecules for Pb^{2+} sorption process. Sorption isotherm shapes of Cd^{2+} and Cu^{2+} were as same as that of Pb^{2+}, indicating a similar

sorption process. The sorption isotherms of Pb^{2+}, Cd^{2+} and Cu^{2+} on NaX zeolite films at different temperature are also presented in Fig. 3. It appeared that sorption isotherm was the highest at 45°C and the lowest at 25°C, which indicated an endothermic nature of the sorption process.

3.4. Sorption time

The effect of sorption time on the sorption capacities of Pb^{2+}, Cd^{2+} and Cu^{2+} on NaX zeolite films, compared with pelletized NaX zeolite particles, was illustrated in Fig. 5. A two-stage kinetic pattern [38] was observed for sorption of three kinds of heavy metals on NaX zeolite films. The sorption rate was extremely rapid in the first stage [25], apparently due to both direct sorption on the surface and ion exchange in the channel. In the second stage, the sorption equilibrium of Pb^{2+}, Cd^{2+} and Cu^{2+} was reached after 120 min. While the sorption curves of Pb^{2+}, Cd^{2+} and Cu^{2+} on pelletized NaX zeolite particles showed that sorption capacity gradually increased with sorption time. The reason for this slowly variation could be that sorption sites on the surface of the pelletized zeolite NaX particles were few. The heavy metal ions should diffuse into pelletized particles firstly, then enter into pore of NaX zeolite, exchange with Na^+ at last. The required time to reach maximum sorption was much longer than 480 min.

3.5. Sorption isotherm

The model parameters of Langmuir and Freundlich isotherms for the sorption of Pb^{2+}, Cd^{2+} and Cu^{2+} on NaX zeolite films are summarized in Table 2. The correlation coefficient R^2 of the Langmuir model was closer to 1 than that of the Freundlich model. Therefore, the Langmuir isotherm model was more suitable to describing sorption data of Pb^{2+}, Cd^{2+} and Cu^{2+} on NaX zeolite films, which suggested the applicability of monolayer coverage and the homogeneous surface on the sorbents. This can be explained by the structure of NaX zeolite. The Na^+, balancing charge of tetrahedral-coordinated aluminum in NaX zeolite, provide ion exchange sites (reaction a, X is NaX zeolite; M^{2+} is heavy metal ions). Thus the energy of most ion exchange sites is similar and sorption is monodermic. Moreover, the distribution of ion exchange sites is relatively homogeneous. These accord with hypothetical condition of Langmuir isotherm model.

$$X–Na^+ + M^{2+} \leftrightarrow X – M^{2+} + Na^+ \qquad (a)$$

According to Table 2, the saturated sorption capacities Q_0 (mmol/g) of Pb^{2+}, Cd^{2+} and Cu^{2+} on NaX zeolite films were 3.075, 2.992 and 2.274 mmol/L at 45°C, respectively. High saturated sorption capacities of Pb^{2+}, Cd^{2+} and Cu^{2+} on NaX zeolite films could be attributed to surface sorption and ion exchange. External surface area of NaX zeolite film is finite and sorption is monodermic. Therefore, the high saturated sorption capacities of Pb^{2+}, Cd^{2+} and Cu^{2+} on NaX zeolite film was mainly caused by ion exchange between heavy metals ions and Na^+ in the channels and cavities of NaX zeolite. Saturated sorption capacity of heavy metals on NaX zeolite films followed the order of Q_0 (Pb^{2+}) > Q_0 (Cd^{2+}) > Q_0 (Cu^{2+}). The difference in saturated sorption capacities
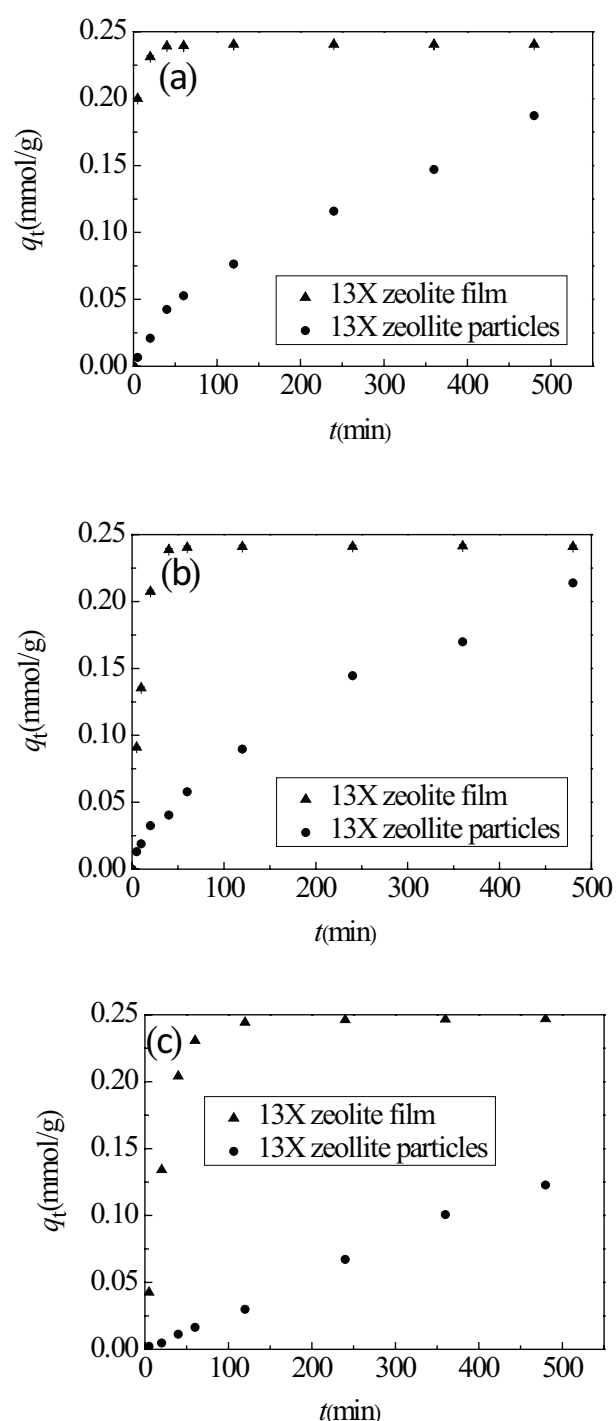

Fig. 5. Sorption capacities of films and pelletized particles for Pb^{2+} (a), Cd^{2+} (b) and Cu^{2+} (c) in different sorption time (T = 25°C, S/L = 0.2 g/L, C_0 = 0.05 mmol/L and pH = 5).

of heavy metals might be influenced by hydration energy, hydrolysis constant, electronegativity, and hydroxide solubility product of the metals [39,40].

Table 2 shows that the saturated sorption capacity of NaX zeolite films increased with temperature. It has been understood that a portion of the water molecules in the

Table 2
Model parameters of Langmuir and Freundlich models

Heavy metal ions	Temperature	Langmuir model			Freundlich model		
		R^2	Q_0/(mmol/g)	b/(L/g)	R^2	n	K_F/[(mmol/g)(L/mmol)^n]
Pb^{2+}	25°C	0.9817	2.822	4.749	0.9585	0.325	1.085
	35°C	0.9845	2.962	4.625	0.9630	0.317	1.081
	45°C	0.9864	3.075	4.652	0.9667	0.309	1.076
Cd^{2+}	25°C	0.9811	2.738	3.927	0.9799	0.482	2.274
	35°C	0.9772	2.869	4.010	0.9771	0.469	2.372
	45°C	0.9900	2.992	4.578	0.9783	0.489	2.644
Cu^{2+}	25°C	0.9738	1.683	5.309	0.9501	0.384	1.421
	35°C	0.9683	1.913	5.012	0.9412	0.415	1.628
	45°C	0.9747	2.274	4.224	0.9571	0.437	1.853

Table 3
Some properties parameters of metals [41]

Ion type	Diameter of crystal ion (nm)	Diameter of ion hydrated sphere (nm)	Hydration energy (kJ/mol)	Electronegativity	Diffusion coefficient cm²·s⁻¹ at 25°C
Pb^{2+}	0.264	0.802	−1481	2.33	0.930×10^{-5}
Cd^{2+}	0.194	0.852	−1816	1.70	0.721×10^{-5}
Cu^{2+}	0.144	0.838	−2121	1.90	0.714×10^{-5}

first hydration shell is tightly bound with the ion during diffusion [42], when the attachment of water molecules to the cation has a lifetime that normally ranges from several picoseconds to tens of picoseconds [18,43]. Hydrated ion diameters of Pb^{2+}, Cd^{2+} and Cu^{2+} are 0.802 nm, 0.852 nm and 0.838 nm respectively (Table 3), while pore size of NaX zeolite is only 0.8 nm [30]. Heavy metal hydration ions could not directly diffuse into channel of NaX zeolite due to effect of size-exclusion [44–46]. However, the heavy metal hydration ions can partially dehydrate, and diffuse into the channel of NaX zeolite to exchange with Na^+ (reaction b, M^{2+} is heavy metal ions). Increasing temperature is conducive to dissociation of heavy metal hydration ions because their dissociation is an endothermic process. The sorption of heavy metal ions onto NaX zeolite film further promoted the dissociation of heavy metal hydration ions. Therefore, High temperature was favorable for the sorption of heavy metals on NaX zeolite film. It further illustrated that sorption of heavy metal ions on NaX zeolite film was mainly based on ion exchange.

$$M^{2+}(H_2O)_n \leftrightarrow M^{2+} + nH_2O \qquad (b)$$

3.6. Sorption kinetics

The sorption process of heavy metal ions on NaX zeolite films and pelletized NaX zeolite particles belongs to liquid-solid sorption process. To analyze influence of adsorbent shape on sorption process and understand sorption mechanism, sorption kinetic models including two main types: reaction-based models and diffusion-based model, are applied to simulate the experimental data in Fig. 5.

3.6.1. Reaction-based models

The calculated curves according to the Lagergren pseudo-first-order and Lagergren pseudo-second-order kinetic models had been plotted together with the experimental data of films and pelletized particles in Fig. 6. The kinetic parameters and correlation coefficients are tabulated in Table 4. As the correlation coefficients were above 0.99, the Lagergren pseudo-second-order kinetic model provided the best correlation for the data of NaX zeolite films, suggesting that sorption kinetics of Pb^{2+}, Cd^{2+} and Cu^{2+} might be controlled by chemical sorption [25,47,48] which was usually associated with significant sharing or exchange of electrons between the adsorbent and adsorbate. Sorption rate with the order of Pb^{2+} > Cd^{2+} > Cu^{2+}, in proportion to kinetic sorption rate constant, might be influenced by their hydration energy and diffusion coefficient (Table 3) because sorption rate of heavy metals increases with decline of hydration energy and rise of diffusion coefficient. While, sorption data of Pb^{2+}, Cd^{2+} and Cu^{2+} on pelletized NaX zeolite particles were more consistent with Lagergren pseudo-first-order kinetic model, indicating that sorption processes could be impeded by intraparticle diffusion. Furthermore, it is noted that kinetic sorption rate constant k_2 of film was much higher than k_2 of particle. Therefore, the sorption rate of heavy metal ions on NaX zeolite films was significantly higher than that on pelletized NaX zeolite particles, which could be contributed to larger surface area and higher utilization rate of NaX zeolite films.

3.6.2. Diffusion-based model

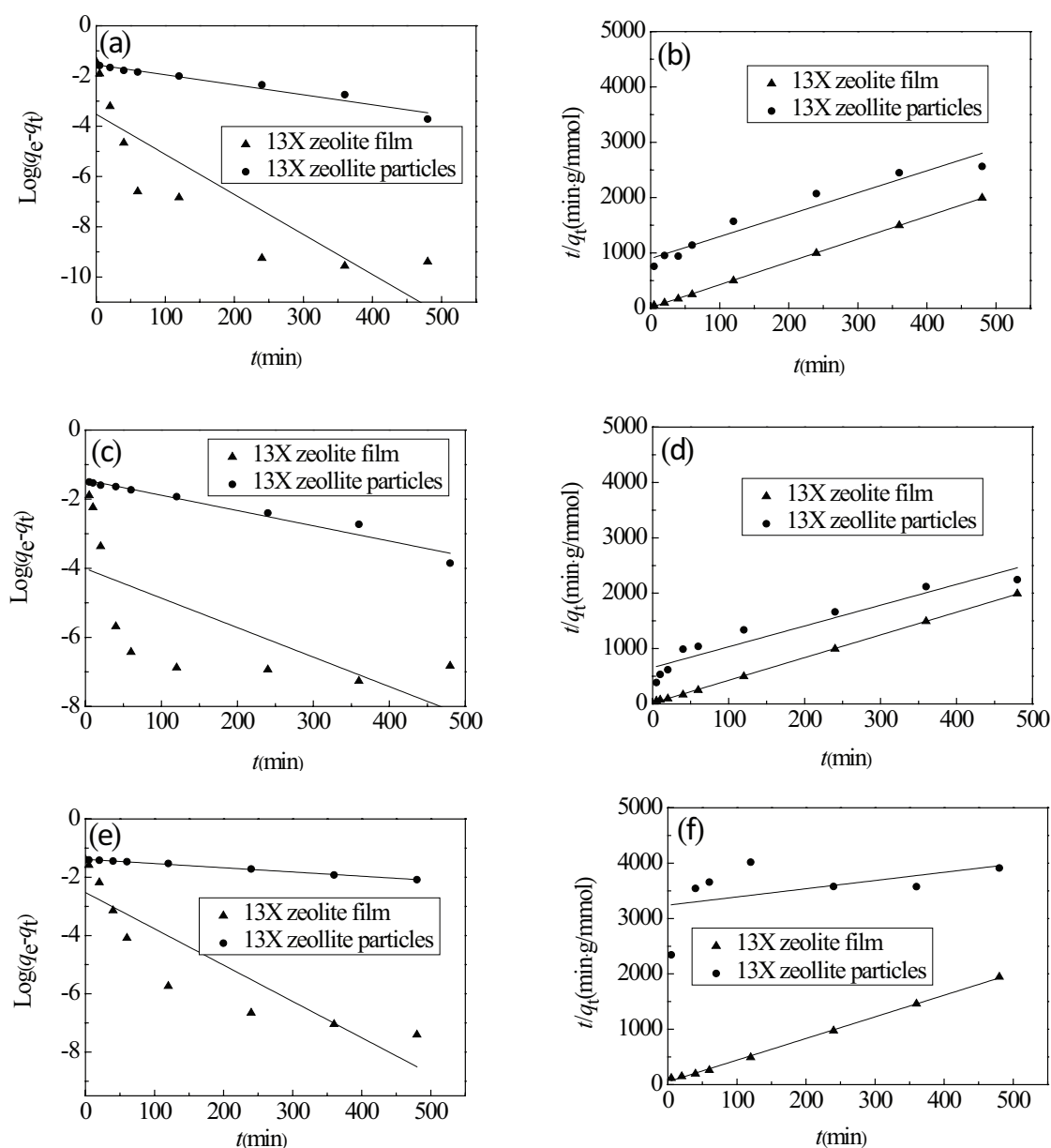It is known that the mechanism of ion exchange can be explained by external mass transfer, intraparticle diffusion

Fig. 6. Pseudo-first-order and Pseudo-second-order model plots of Pb^{2+} (a, b), Cd^{2+} (c, d) and Cu^{2+} (e, f) sorption by NaX zeolite films and pelletized NaX zeolite particles (T = 25°C, S/L = 0.2 g/L, C_0 = 0.05 mmol/L and pH = 5).

Table 4
Lagergren pseudo-first-order and Lagergren pseudo-second-order model parameters for sorption of Pb^{2+}, Cd^{2+} and Cu^{2+} on NaX zeolite films and pelletized particles

| Heavy metal	NaX zeolite	Lagergren pseudo-first-order kinetic model			Lagergren pseudo-second-order kinetic model		
		R^2	q_{e1}/(mmol/g)	k_1/min^{-1}	R^2	q_{e2}/(mmol/g)	k_2/[g/(mmol·min)]
Pb^{2+}	Film	0.7069	0.030	0.016	0.9998	0.2428	1.180
	Particle	0.9550	0.213	0.004	0.9361	0.2522	0.017
Cd^{2+}	Film	0.3897	0.018	0.009	0.9997	0.2438	1.042
	Particle	0.9539	0.236	0.004	0.9058	0.2662	0.022
Cu^{2+}	Film	0.7842	0.080	0.012	0.9984	0.2559	0.294
	Particle	0.9955	0.250	0.001	0.0830	0.6738	0.001
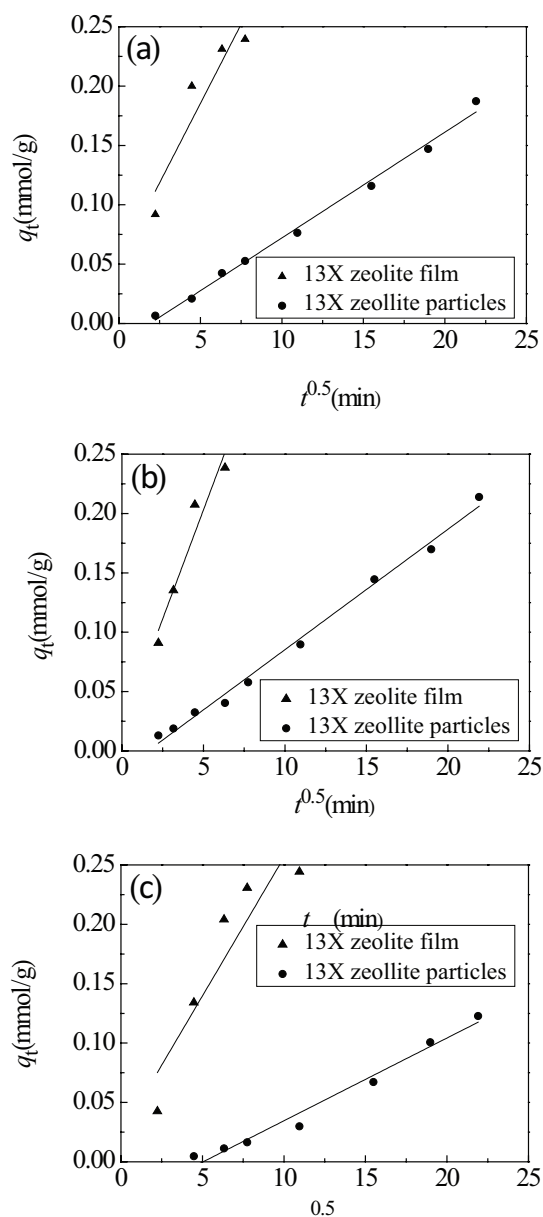
Fig. 7. Weber and Morris model sorption spots of Pb^{2+} (a), Cd^{2+} (b) and Cu^{2+} (c) on NaX zeolite films and pelletized NaX zeolite particles (T = 25°C, S/L = 0.2 g/L, C_0 = 0.05 mmol/L and pH = 5).

or chemical exchange [13]. Chemical exchange generally rapidly occurs, so the slower external mass transfer and intraparticle diffusion are mainly considered as rate limiting steps [26].

Weber and Morris model sorption spots of Pb^{2+}, Cd^{2+} and Cu^{2+} on NaX zeolite films and pelletized NaX zeolite particles are shown in Fig. 7, and the parameters for Weber and Morris model are summarized in Table 5. The result suggested that Weber and Morris model was not effective in describing the sorption data of NaX zeolite films except equilibrium state where sorption capacity almost didn't change [39]. So intraparticle diffusion was not considered as the rate-limiting step during the sorption process. While, Weber and Morris model showed excellent correlation with the sorption data of Pb^{2+}, Cd^{2+} and Cu^{2+} on pelletized NaX zeolite particles. The straight line didn't pass through the origin, indicating that both external mass transfer and intraparticle diffusion were considered as rate-limiting steps. This might be attributed to small contact surface area and diffusion of heavy metals in particles. Obviously, It could be found that K_{WM} of NaX zeolite films is higher than K_{WM} of pelletized NaX zeolite particles, when the values of K_{WM} (film)/K_{WM} (particle) for Pb^{2+}, Cd^{2+} and Cu^{2+} were 3.00, 3.63 and 3.32 respectively, showing high diffusion rate of heavy metal ions onto NaX zeolite films. The results indicated NaX zeolite film can effectively avoid the effect of diffusion resistance caused by particle morphology due to increasing external surface area.

4. Conclusions

In this study, continuous NaX zeolite films on α-Al_2O_3 ceramic tube were successfully prepared by pre-coating sol, drying in warm temperature and crystallizing in synthetic solution. This method avoids preparation process of crystal seed.

The NaX zeolite film exhibited high saturated sorption capacity and sorption rate for Pb^{2+}, Cd^{2+} and Cu^{2+}. Sorption capacity of the NaX zeolite film increased with temperature.

The Langmuir isotherms model was better applied to describe sorption equilibrium data of Pb^{2+}, Cd^{2+}, and Cu^{2+} on NaX zeolite films than Freundlich isotherms model, which showed applicability of monolayer coverage and the homogeneous surface on the sorbents.

The pseudo-second-order kinetic model was appropriate to describe the sorption kinetic performance of NaX

Table 5
Weber and Morris model parameters for sorption of Pb^{2+}, Cd^{2+} and Cu^{2+} on NaX zeolite films and pelletized NaX zeolite particles

Heavy metal	NaX zeolite	Weber and Morris model			
		R^2	I	$K_{WM}/$ (mmol·g^{-1}·min$^{-0.5}$)	K_{WMI} (film)/ K_{WM} (particle)
Pb^{2+}	Films	0.8176	0.0518	0.0267	3.00
	Particles	0.9926	−0.0169	0.0089	
Cd^{2+}	Films	0.9057	0.0195	0.0367	3.63
	Particles	0.9924	−0.0162	0.0101	
Cu^{2+}	Films	0.8021	0.0231	0.0233	3.32
	Particles	0.9740	−0.0351	0.0070	

zeolite films. While, sorption data of the pelletized NaX zeolite particles were better consistent with Lagergren pseudo-first-order kinetic model.

Weber and Morris model indicated the NaX zeolite film can effectively avoid the effect of diffusion resistance caused by particle morphology due to increasing external surface area.

Overall, NaX zeolite films from this work could well be used as a high performance sorbent in the treatment of heavy metal containing wastewater.

Acknowledgments

References

[1] Y. Yurekli, Removal of heavy metals in wastewater by using zeolite nano-particles impregnated polysulfone membranes, J. Hazard. Mater., 309 (2016) 53–64.

[2] G.P.C. Rao, S. Satyaveni, A. Ramesh, K. Seshaiah, K.S.N. Murthy, N.V. Choudary, Sorption of cadmium and zinc from aqueous solutions by zeolite 4A, zeolite 13X and bentonite, J. Environ. Manage., 81(3) (2006) 265–272.

[3] C. Li, H. Zhong, S. Wang, J. Xue, Z. Zhang, A novel conversion process for waste residue: synthesis of zeolite from electrolytic manganese residue and its application to the removal of heavy metals, Colloids Surf. A: Physicochem. Eng. Asp., 470 (2015) 258–267.

[4] S.A. Kim, S. Kamala-Kannan, K.J. Lee, Y.J. Park, P.J. Shea, W.H. Lee, H.M. Kim, B.T. Oh, Removal of Pb(II) from aqueous solution by a zeolite-nanoscale zero-valent iron composite, Chem. Eng. J., 217 (2013) 54–60.

[5] W. Bao, L. Liu, H. Zou, S. Gan, X. Xu, G. Ji, G. Gao, K. Zheng, Removal of Cu^{2+} from aqueous solutions using Na-A zeolite from oil shale ash, Chinese J. Chem. Eng., 21(9) (2013) 974–982.

[6] B. Xie, C. Shan, Z. Xu, X. Li, X. Zhang, J. Chen, B. Pan, One-step removal of Cr(VI) at alkaline pH by UV/sulfite process: reduction to Cr(III) and in situ Cr(III) precipitation, Chem. Eng. J., 308 (2017) 791–797.

[7] X. Kong, Z. Han, W. Zhang, L. Song, H. Li, Synthesis of zeolite-supported microscale zero-valent iron for the removal of Cr^{6+} and Cd^{2+} from aqueous solution, J. Environ. Manage., 169 (2016) 84–90.

[8] H. Luo, G. Liu, R. Zhang, Y. Bai, S. Fu, Y. Hou, Heavy metal recovery combined with H_2 production from artificial acid mine drainage using the microbial electrolysis cell, J. Hazard. Mater., 270 (2014) 153–159.

[9] J. Zhang, X. Liu, X. Chen, J. Li, Z. Zhao, Separation of tungsten and molybdenum using macroporous resin: competitive adsorption kinetics in binary system, Hydrometallurgy, 144–145 (2014) 77–85.

[10] Y. Jin, Y. Wu, J. Cao, Y Wu, Adsorption behavior of Cr(VI), Ni(II), and Co(II) onto zeolite 13X, Desal. Water Treat., 54(2) (2015) 511–524.

[11] Y. Zheng, D. Huang, A. Wang, Chitosan-g-poly(acrylic acid) hydrogel with crosslinked polymeric networks for Ni^{2+} recovery, Anal. Chim. Acta., 687(2) (2011) 193–200.

[12] M.A. Barakat, New trends in removing heavy metals from industrial wastewater, Arab. J. Chem., 4(4) (2011) 361–377.

[13] D. Nibou, H. Mekatel, S. Amokrane, M. Barkat, M. Trari, Adsorption of Zn^{2+} ions onto NaA and NaX zeolites: kinetic, equilibrium and thermodynamic studies, J. Hazard. Mater., 173(1–3) (2010) 637–646.

[14] M. Deravanesiyan, M. Beheshti, A. Malekpour, Alumina nanoparticles immobilization onto the NaX zeolite and the removal of Cr (III) and Co (II) ions from aqueous solutions, J. Ind. Eng. Chem., 21 (2015) 580–586.

[15] M.A.S.D. Barros, E.A. Silva, P.A. Arroyo, C.R.G. Tavares, R.M. Schneider, M. Suszek, E.F. Sousa-Aguiar, Removal of Cr (III) in the fixed bed column and batch reactors using as adsorbent zeolite NaX, Chem. Eng. Sci., 59(24) (2004) 5959–5966.

[16] F. Pepe, B.D. Gennaro, P. Aprea, D. Caputo, Natural zeolites for heavy metals removal from aqueous solutions: modeling of the fixed bed Ba^{2+}/Na^{+} ion-exchange process using a mixed phillipsite/chabazite-rich tuff, Chem. Eng. J., 219 (2013) 37–42.

[17] A. Mundstock, N. Wang, S. Friebe, J. Caro, Propane/propene permeation through Na-X membranes: the interplay of separation performance and pre-synthetic support functionalization, Micropor. Mesopor. Mat., 215 (2015) 20–28.

[18] L. Lia, J. Dong, T.M. Nenoff, R. Lee, Reverse osmosis of ionic aqueous solutions on a MFI zeolite membrane, Desalination, 170(3) (2004) 309–316.

[19] M. Matsukata, E. Kikuchi, Zeolitic membranes: Synthesis, properties, and prospects, B. Chem. Soc. Jpn., 70(10) (1997) 2341–2356.

[20] X. Xu, Y. Bao, C. Song, W. Yang, J. Liu, L. Lin, Microwave-assisted hydrothermal synthesis of hydroxy-sodalite zeolite membrane, Micropor. Mesopor. Mat., 75(3) (2004) 173–181.

[21] H. Kita, K. Fuchida, T. Horita, H. Asamura, K. Okamoto, Preparation of Faujasite membranes and their permeation properties, Sep. Purif. Technol., 25(1–3) (2001) 261–268.

[22] S. Aghazadeh, E. Safarzadeh, M. Gharabaghi, M. Irannajad, Modification of natural zeolite for Cu removal from waste waters, Desal. Water Treat., 57(57) (2016) 1–8.

[23] H. Freundlich, Adsoption in solution, Phys. Chem., 57 (1906) 384–401.

[24] X. Yang, S. Yang, S. Yang, J. Hu, X. Tan, X, Wang. Effect of pH, ionic strength and temperature on sorption of Pb(II) on NKF-6 zeolite studied by batch technique, Chem. Eng. J., 168(1) (2011) 86–93.

[25] U. Habiba, A.M. Afifi, A. Salleh, B.C. Ang, Chitosan/(polyvinyl alcohol)/zeolite electrospun composite nanofibrous membrane for adsorption of Cr^{6+}, Fe^{3+} and Ni^{2+}, J. Hazard. Mater., 322 (2017) 182–194.

[26] M. Çanli, Y. Abali, A novel Turkish natural zeolite (clinoptilolite) treated with hydrogen peroxide for Ni^{2+} ions removal from aqueous solutions, Desal. Water Treat., 57(15) (2016) 6925–6935.

[27] J. Aguado, J.M. Arsuaga, A. Arencibia, M. Lindo, V. Gascón, Aqueous heavy metals removal by adsorption on amine-functionalized mesoporous silica, J. Hazard. Mater., 163(1) (2009) 213–221.

[28] B. Acemioğlu, Batch kinetic study of sorption of methylene blue by perlite, Chem. Eng. J., 106(1) (2005) 73–81.

[29] M.H. Kalavathy, T. Karthikeyan, S. Rajgopal, L.R. Miranda, Kinetic and isotherm studies of Cu(II) adsorption onto H_3PO_4-activated rubber wood sawdust, J. Colloid Interf. Sci., 292(2) (2005) 354–362.

[30] Y.S. Al-Degs, M.I. El-Barghouthi, A.A. Issa, M.A. Khraisheh, G.M. Walker, Sorption of Zn(II), Pb(II), and Co(II) using natural sorbents: equilibrium and kinetic studies, Water Res., 40(14) (2006) 2645–2658.

[31] S.S. Gupta, K.G. Bhattacharyya, Kinetics of adsorption of metal ions on inorganic materials: A review, Adv. Colloid Interfac., 162(1–2) (2011) 39–58.

[32] The International Zeolite Association. http://asia.iza-structure.org/IZA-SC/mat_xrd.php?STC=FAU&ID=FAU_1/, 2017 (accessed 17.08.13).

[33] G. Zhu, Y. Li, H. Zhou, J. Liu, W. Yang, Microwave synthesis of high performance FAU-type zeolite membranes: Optimization, characterization and pervaporation dehydration of alcohols, J. Membr. Sci., 337(1–2) (2009) 47–54.

[34] S.T. Akar, S. Arslan, T. Alp, D. Arslan, T. Akar, Biosorption potential of the waste biomaterial obtained from cucumis melo for the removal of Pb^{2+} ions from aqueous media: equilibrium, kinetic, thermodynamic and mechanism analysis, Chem. Eng. J., 185–186 (2012) 82–90.

[35] D. Karadag, Y. Koc, M. Turan, B, Armagan. Removal of ammonium ion from aqueous solution using natural turkish clinoptilolite, J. Hazard. Mater., 136(3) (2006) 604–609.

[36] R. Leyva-Ramos, G. Aguilar-Armenta, L.V. Gonzalez-Gutierrez, R.M. Guerrero-Coronado, J. Mendoza-Barron, Ammonia exchange on clinoptilolite from mineral deposits located in mexico, J. Chem. Technol. Biot., 79(6) (2004) 651–657.

[37] C.H. Giles, D. Smith, A. Huitson, A general treatment and classification of the solute adsorption isotherm I. theoretical, J. Colloid Interf. Sci., 47(3) (1974) 755–765.

[38] E.S.Z. El-Ashtoukhy, N.K. Amin, O. Abdelwahab, Removal of lead (II) and copper (II) from aqueous solution using pomegranate peel as a new adsorbent, Desalination, 223 (1–3) (2008) 162–173.

[39] T.C. Nguyen, P. Loganathan, T.V. Nguyen, S. Vigneswaran, J. Kandasamy, R. Naidu, Simultaneous adsorption of Cd, Cr, Cu, Pb, and Zn by an iron-coated Australian zeolite in batch and fixed-bed column studies, Chem. Eng. J., 270 (2015) 393–404.

[40] M. Minceva, R. Fajgar, L. Markovska, V. Meshko, Comparative study of Zn^{2+}, Cd^{2+}, and Pb^{2+} removal from water solution using natural clinoptilolitic zeolite and commercial granulated activated carbon. Equilibrium of adsorption, Sep. Sci. Technol., 43(8) (2008) 2117–2143.

[41] S. Ricordel, S. Taha, I. Cisse, G. Dorange, Heavy metals removal by adsorption onto peanut husks carbon: characterization, kinetic study and modeling, Sep. Purif. Technol., 24(3) (2001) 389–401.

[42] M.Y. Kiriukhin, K.D. Collins, Dynamic hydration numbers for biologically important ions, Biophys. Chem., 99(2) (2002) 155–168.

[43] G.W. Neilson, J.E. Enderby, The coordination of metal aquaions, Adv. Inorg. Chem., 34 (1989) 195–218.

[44] L. Li, J. Dong, T.M. Nenoff, R. Lee, Desalination by reverse osmosis using MFI zeolite membranes, J. Membr. Sci., 243(1–2) (2004) 401–404.

[45] L. Li, J. Dong, T.M. Nenoff, Transport of water and alkali metal ions through MFI zeolite membranes during reverse osmosis, Sep. Purif. Technol., 53(1) (2007) 42–48.

[46] X. Zou, G. Zhu, H. Guo, X. Jing, D. Xu, S. Qiu, Effective heavy metal removal through porous stainless-steel-net supported low siliceous zeolite ZSM-5 membrane, Micropor. Mesopor. Mater., 124(1–3) (2009) 70–75.

[47] Y.S. Ho, G. Mckay, Pseudo-second order model for sorption processes, Process Biochem., 34(5) (1999) 451–465.

[48] W. Plazinski, W. Rudzinski, A. Plazinska, Theoretical models of sorption kinetics including a surface reaction mechanism: a review, Adv. Colloid Interfac., 152(1–2) (2009) 2–13.